Supplemental Information

in situ polymer gelation in confined flow controls intermittent dynamics

Barrett T. Smith and Sara M. Hashmi

Department of Chemical Engineering, Northeastern University

January 10, 2024

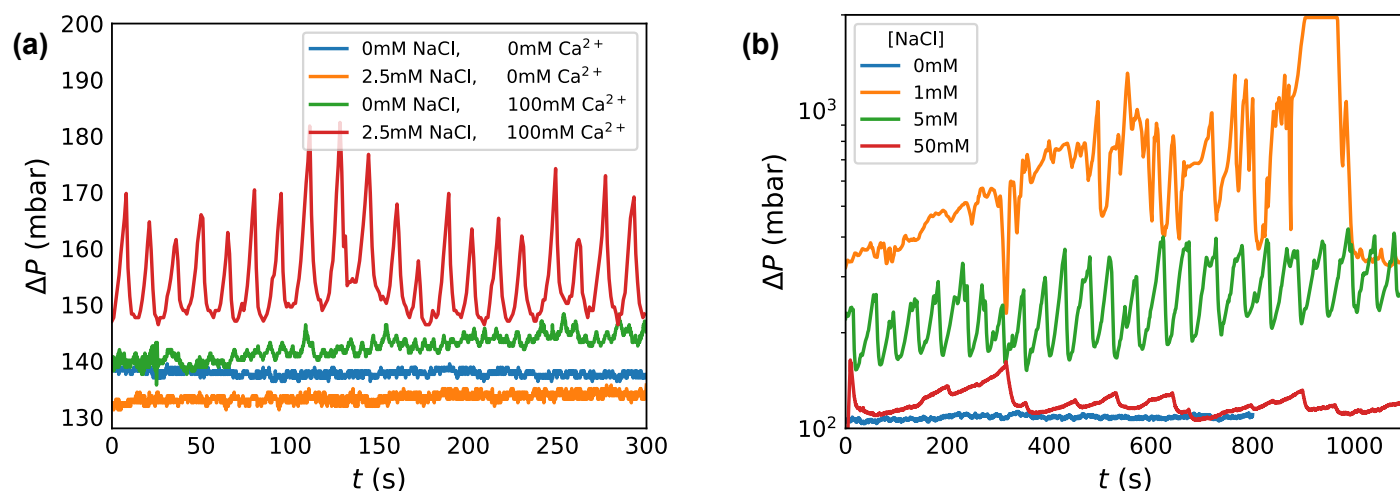## 1 Intermittent dynamics require alginate, calcium and sodium

Figure 1: Both sodium and calcium are required to crosslink alginate in flow. (a) The four traces represent pressure traces with combinations of sodium and calcium ions, with $C_{NaCl} = C_{Ca^{2+}} = 0$ mM in blue, $C_{NaCl} = 2.5$mM and $C_{Ca^{2+}} = 0$mM in orange, $C_{NaCl} = 0$ mM and $C_{Ca^{2+}} = 100$ mM in green, and $C_{NaCl} = 2.5$mM and $C_{Ca^{2+}} = 100$ mM in red. Only the red trace, in which the system contains both ions, exhibits regular peaks in $\Delta P(t)$. These flow tests are conducted at $Q_T = 2.4\mu$L/min.(b) While sodium chloride is necessary for clogging to occur, the magnitude of the pressure peaks decreases with increases in sodium chloride. The y-axis is on a log scale to emphasize the difference between 0 and 50mM sodium chloride. Data is collected at $C_{Alg} = 0.1$mg/mL, $C_{Ca^{2+}} = 100$ mM, $Q_T = 1.2\mu$L/min.

Even though alginate forms a gel in quiescence simply with the addition of calcium, we find that the intermittent gelation, deposition and ablation in flow also requires sodium chloride, as seen in Fig. 1. Fig. 1a shows the $\Delta P(t)$ behavior that results from mixing the alginate stream with an aqueous stream using different combinations of salts. The aqueous stream contains either no salt, sodium chloride only, CaCl$_2$ only, or both sodium chloride and CaCl$_2$. Each of these 4 conditions is shown in Fig. 2a. When calcium is absent, alginate does not gel. $\Delta P(t)$ remains constant when alginate mixes with water either with or without added sodium chloride, as seen in the blue ($C_{NaCl} = 0$ mM) and orange ($C_{NaCl} = 2.5$ mM) data traces. Adding calcium in the absence of sodium chloride results in small, high frequency pressure peaks, as shown in green ($C_{Ca^{2+}} = 100$ mM and $C_{NaCl} = 0$ mM). These peaks correspond to small depositions that rapidly clear. While observable under the microscope, these small deposits do not significantly impede flow. Rather, they cause fluctuations in driving pressure of <5mbar which occur around every 5s, a time scale which approaches the 2s response time of the pump. Significant deposition and intermittent clogging emerges only when sodium chloride is added, even in small quantities, as seen in the red trace, with $C_{Ca^{2+}} = 100$ mM and $C_{NaCl} = 2.5$ mM.

Interestingly, the effect of additional sodium ions is non-monotonic, as seen in Fig. 1. All four traces represent flow tests with $C_{Ca^{2+}} = 100$ mM and varying concentrations of sodium chloride. Little deposition is seen without sodium chloride, shown in the blue trace, which corresponds to the green trace in Fig. 2a. Small amounts of sodium chloride, $C_{NaCl} = 1$ mM, lead to significant deposition and occlusion of the channel, seen in red, but without much regularity to the ablation behavior. An increased uniformity of the deposition/ablation behavior emerges at slightly higher concentrations of sodium

chloride, and at somewhat lower levels of occlusion, as inferred from the smaller increase in pressure drop required before the clog ablates. Further increasing the sodium chloride concentration results in even smaller features in ΔP, more similar in scale to the features present in the absence of sodium chloride.

It is worth noting that the sodium chloride must be present in the alginate stream to obtain the behaviors seen in the red trace in Fig. 1, and the orange, green and red traces in Fig. 1b. Adding sodium to the calcium stream alone does not produce significant deposition. However, the calcium stream does not require sodium chloride for there to be significant deposition. To reduce differences between the two inlet streams while exploring dependence of intermittency on C_{Alg} and $C_{Ca^{2+}}$, a proportional concentration of sodium chloride is included in both solutions for all experimental conditions listed in Table 1, namely a ratio of $C_{NaCl} = 2.5$mM to $C_{Alg} = 0.1$mg/mL.

The necessary requirement of sodium to enable intermittent alginate gel deposition suggests that sodium counterion interaction with alginate polymers plays an important role in the formation of the gel. Positively charged sodium ions act as counterions for the negatively charged alginate polymer. In bulk alginate gels, sodium counterion binding to alginate polymers reduces the electrostatic repulsion between negatively charged alginate polymers, allowing for greater flexibility in the polymer chain and faster gelation kinetics [1, 2]. The non-monotonic effect of sodium seen in Fig. 1b shows that excess sodium reduces both the extent of deposition and frequency of ablation in flowing alginate. A small degree of counterion binding to alginate may enable gelation in flow and thus, facilitate deposition. At the same time, sodium chloride also weakens alginate gels, which may correlate with the decreasing size of the pressure peaks as sodium concentration increases [2, 3].

2 Reproducibility across different devices

Replicate channels with the same design exhibit slightly different deposition/ablation behavior in flow tests done at constant conditions. SI Fig. 2 compares the dynamics of $C_{Alg} = 0.1$mg/mL mixed with $C_{Ca^{2+}} = 100$ mM flowed at $Q_T = 1.2\mu$L/min through six different devices. The plot shows the size of the pressure peak at ablation $\Delta P - \Delta P_0$ as a function of the peak-to-peak time interval Δt. Each data point represents a single ablation event. The build up of alginate as measured by the change in driving pressure vs. the time to ablation is fairly consistent in each device. There is significant overlap in the data obtained from Device 4 (red) and 5 (purple) and in the data obtained from Device 3 (green) and 6 (brown). Despite the apparent differences in the data obtained from Device 1 (blue) and 2 (orange), this degree of variation does not approach the differences observed at different flow conditions. When considering all six devices, the absolute difference in driving pressure ranges from ~10-350 mbar, and the time to ablation varies from ~35-120s.

Importantly, there is a much greater degree of variation between flow tests using different reaction conditions than that observed between flow tests at the same conditions obtained from different devices. SI Fig. 3 shows the same scatter plot of $\Delta P - \Delta P_0$ vs. Δt for four different calcium concentrations when $C_{Alg} = 0.1$mg/mL. The data from all six devices shown in SI Fig. 2 are all shown in green in SI Fig 3. The comparison with different calcium concentrations clearly shows that different reaction conditions result in separate populations of ablation events.
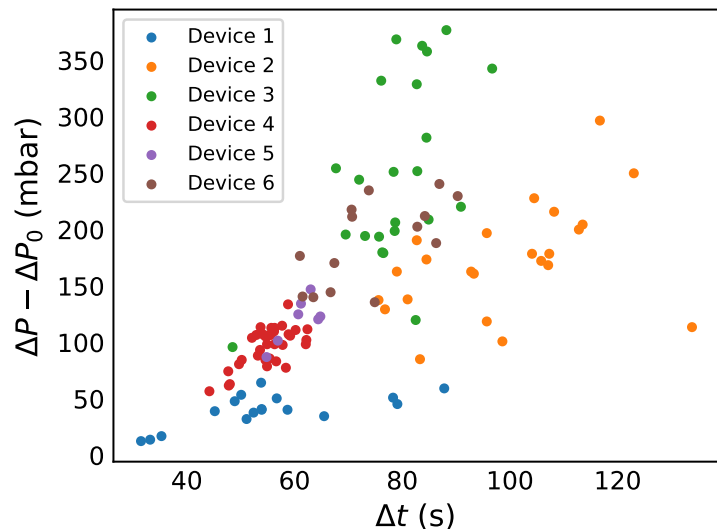

Figure 2: Device-to-device variation: The difference between the driving pressure at the point of greatest occlusion baseline pressure is plotted as a function of the time interval between ablation events. Each data point represents a single ablation event. Each color represents a separate device of the same design. Comparison of results from six different devices shows that replicate devices result in slightly different deposition/ablation patterns. Data is taken at $C_{Alg} = 0.1$mg/mL, $C_{Ca^{2+}} = 100$ mM, $Q_T = 1.2\mu$L/min.
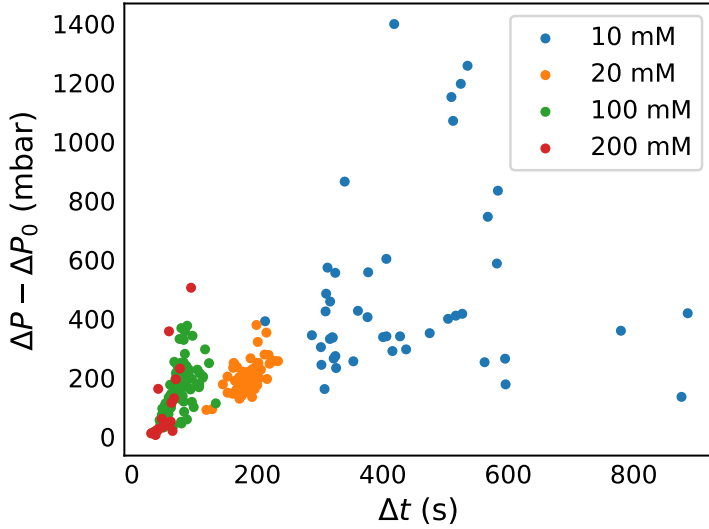
Figure 3: Variation between reaction conditions: The difference between the driving pressure at the point of greatest occlusion baseline pressure is plotted as a function of the time interval between ablation events. Four different calcium concentrations are shown, with fixed $C_{Alg} = 0.1\text{mg/mL}$ and $Q_T = 1.2\mu\text{L/min}$. All data from SI Fig. 2 are plotted in green. The difference between conditions is larger than the difference between devices.

3   Surface chemistry of the microfluidic channels

As part of the effort to understand how and where alginate deposits on the walls of the channel, PDMS-based Y-shaped microfluidic devices are prepared on glass slides and on slides coated with a thin layer of PDMS. A comparison of the two reveals very similar behaviors. Fig. 4 shows the behavior $\Delta P(t)$ for flow through a PDMS device adhered to glass as compared to flow through a PDMS device adhered to PDMS-coated glass. The flow conditions are the same in both cases: $C_{Alg} = 0.1\text{mg/mL}$ and $C_{Ca^{2+}} = 100$ mM flowing at $Q_T = 12.0\mu\text{L/min}$. The difference between the two traces of $\Delta P(t)$ is comparable to the differences in flow between any two devices adhered to glass slides, which is shown in Fig. 2. This demonstrates that alginate deposition does not require a glass substrate, nor does alginate deposit on glass significantly differently than it deposits on PDMS.
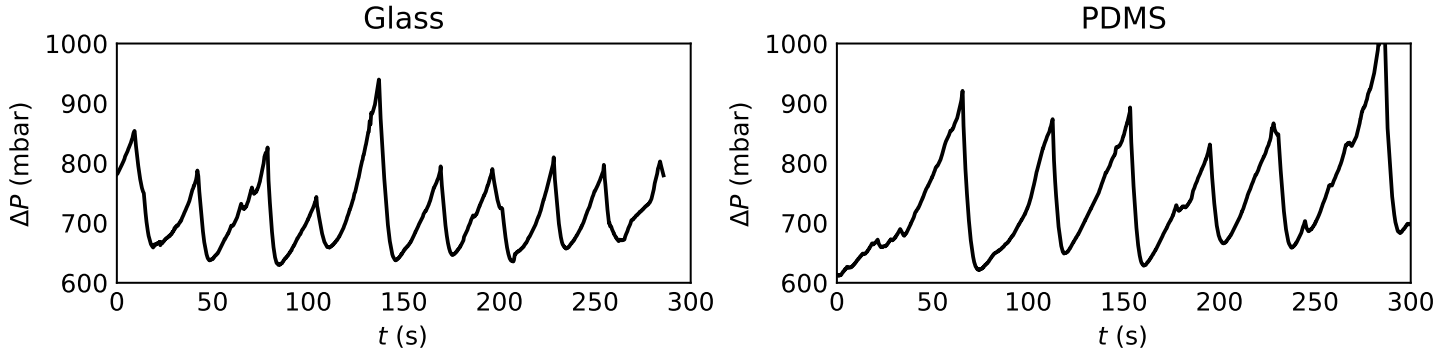

Figure 4: Traces of $\Delta P(t)$ for flow through Y-shaped junctions made of PDMS adhered to glass slides with and without a PDMS coating exhibit similar intermittent flow behavior. This demonstrates that alginate gel clogging is not specific to glass or PDMS. Data is taken at $C_{Alg} = 0.1$ mg/mL, $C_{Ca^{2+}} = 100$ mM, $Q_T = 12.0\mu\text{L/min}$.

In additional experiments, channel chemistry is modified to increase either hydrophilicity or hydrophobicity. Treatment with poly-vinyl alcohol (PVA) is frequently used to increase the hydrophilicity of PDMS devices [4]. The effect of a PVA coating on alginate deposition/ablation can be seen in Fig. 5, where $C_{Alg} = 0.1\text{mg/mL}$ and $C_{Ca^{2+}} = 100$ mM are flowing at $Q_T = 2.4\mu\text{L/min}$ in either a PVA-coated hydrophilic channel (in blue), or a "normal", uncoated, semi-hydrophobic channel (in orange). The frequency of ablation is larger in the hydrophilic channel as compared to the normal channel. Correspondingly, the driving pressure at ablation is much lower in hydrophilic channels.

Aquapel® is a commercial glass treatment commonly used to increase the hydrophobicity of glass and PDMS surfaces [5]. The effect of an Aquapel coating on alginate deposition/ablation can be seen in SI Fig. 5b, where $C_{Alg} = 0.1\text{mg/mL}$ and $C_{Ca^{2+}} = 100$ mM are flowing at $Q_T=6.0\mu\text{L/min}$. Alginate deposition in this device continued beyond the ΔP_{Abl} of the normal device. In fact, no ablation event is observed in the hydrophobic channel. Instead, the PDMS loses adhesion with

the glass at $\Delta P \approx 750$ mbar. The partial delamination is due to the interference of Aquapel with the bonding of the PDMS to the glass.
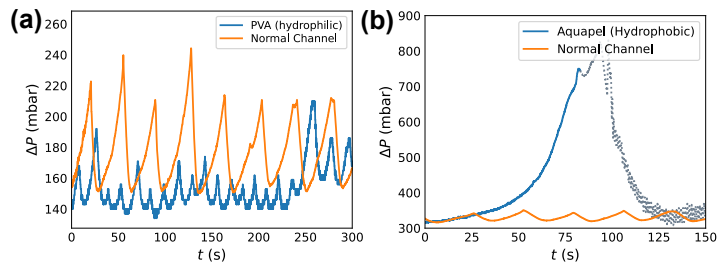

Figure 5: Traces of $\Delta P(t)$ for flow through (a) a hydrophilic PVA-coated channel or (b) a hydrophobically coated channel show changes in feature size versus a channel with no coating. Alginate adheres more stongly to hydrophobic channels, although alginate deposition is seen in all cases. Data is taken at $C_{Alg} = 0.1$ mg/mL, $C_{Ca^{2+}} = 100$ mM. For (a) $Q_T = 2.4\mu$L/min. while for (b) $Q_T = 6.0\mu$L/min. Note: Aquapel coating interferes with the adhesion between the PDMS and glass. As a result, the channel delaminated at ~80 seconds. Data after delamination is plotted as a dotted line.

These surface chemistry experiments demonstrate that alginate gel deposits on the channel wall within a wide range of hydrophobicities. Driving pressure at ablation does vary significantly with channel hydrophobicity. Gels stick more to hydrophobic surfaces: the shear stress required for ablation, as indicated by the driving pressure at ablation, is lower in hydrophilic channels.

4   Flow rate is constant

Gel deposition and ablation events at constant flow rate cause changes in pressure, but flow rate remains constant. During driving pressure spikes, ΔP can increase by a factor of 2 above the baseline for the duration of the deposition event. At the moment of ablation, pressure returns to its baseline value over the course of an average of 10 seconds, though sometimes as many as 30 seconds, as the gel leaves the device entirely. At ablation, the flow rate also experiences a spike while the pressure controller responds to the change of resistance in the channel while working to maintain constant flow rate. However, the spike in flow rate is much smaller in relative magnitude and of shorter duration than the spike in pressure. Q_T spikes by a maximum factor of ~ 40 % while ΔP spikes by more than a factor of 2. Further, flow rate returns to within 10% of the desired flow rate within an average of 5 seconds after ablation. Thus, we consider the flow rate to be constant over the time scale of the deposition/ablation pattern. SI Fig. 6 shows simultaneous traces of Q_T (blue) and ΔP (orange) over the course of six ablation events for conditions $C_{Alg} = 0.1$ mg/mL, $C_{Ca^{2+}} = 100$ mM and $Q_T = 1.2\mu$L/min. The variations in Q_T within the horizontal plateaus while deposition occurs are less than $\sim 0.1\mu$L/min.
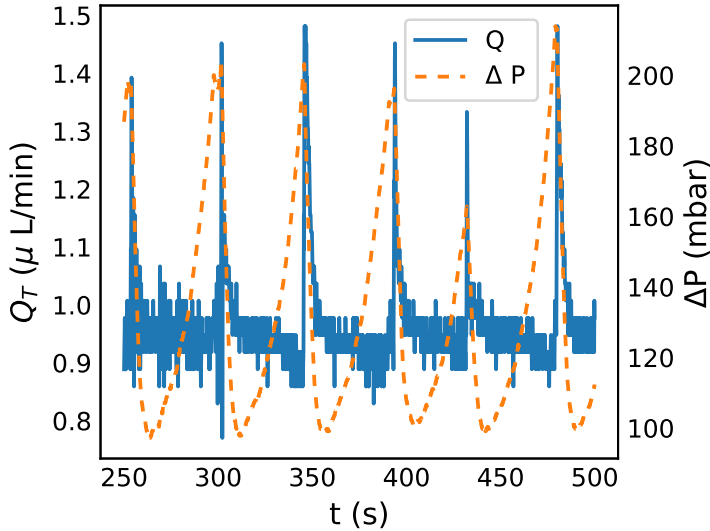
Figure 6: Flow rate varies slightly during clog ablation events. Several seconds are required for the pump to adjust to the decreased flow resistance as a gel clot is removed from the wall and exits the device. However, the magnitude and duration of the flow rate change are small compared to the magnitude in the pressure drop associated with alginate deposition. $Q_T(t)$ is plotted in blue and $\Delta P(t)$ in orange for data taken at $C_{Alg} = 0.1$ mg/mL, $C_{Ca^{2+}} = 100$ mM and $Q_T = 1.2\mu$ L/min.

5   Microscopy images and video

The two supplemental videos are described in the manuscript: both refer to the pressure trace data shown in Fig. 1b, with an appended microscopy video showing the simultaneous deposition and ablation behavior. One supplemental video shows a single deposition/ablation event in real time; the other shows the entire trace sped up by a factor of 5. Both are approximately one minute long.

SI Fig. 7 shows several examples of phase-contrast microscopy images of alginate deposition in microfluidic channels obtained seconds before ablation events. In all images, darker regions within the channel correspond to deposited gel. Images (a)-(d) show that deposition looks similar at different flow rates, from $Q_T = 1.2\mu$L/min in (a) to $Q_T = 12.0\mu$L/min in (d). While there are small differences in the deposition patterns at different flow rates, in all cases the deposit begins at the junction and extends several hundred microns past the junction, and additionally, smaller pieces of gel can be seen further downstream of the main deposit. While the channel walls in (a)-(d) show some micron-scale features in the sidewall, devices with much smoother walls show a similar deposition/ablation pattern, for instance as seen in (e), at $Q_T = 1.2\mu$L/min. Although the image in (e) is obtained under slightly brighter illumination, the deposit extends several hundred microns past the junction, with additional smaller pieces downstream. Thus we conclude that surface roughness on the micron scale is not responsible for, nor required by, the deposition of alginate. For all images, $C_{Alg} = 0.1$ mg/mL and $C_{Ca^{2+}} = 100$ mM.
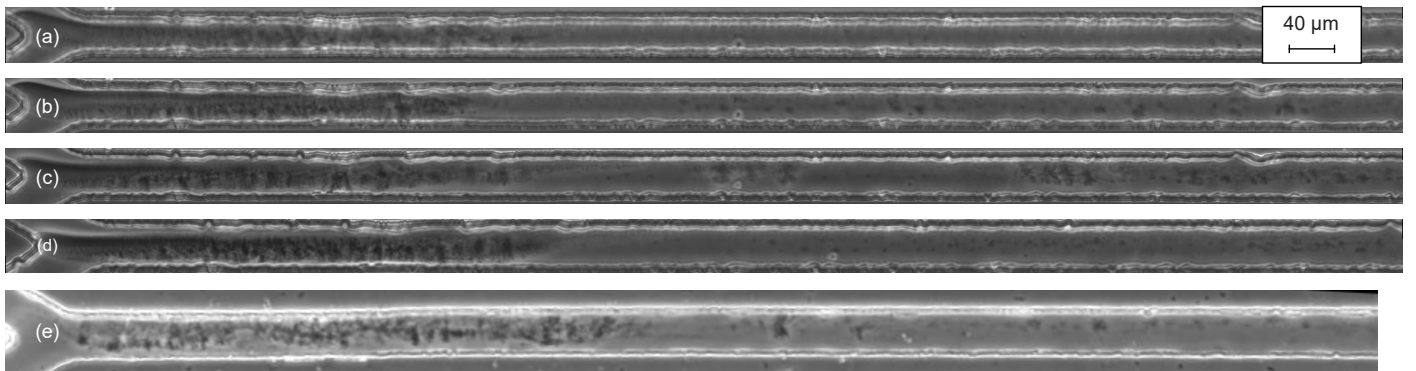

Figure 7: Microscopy images of different deposition events obtained from different devices and conditions. Images (a), (b), (c), and (d) show clogs formed at flow rates $Q_T = 1.2, 2.4, 6.0,$ and 12.0 μL/min, respectively. Microscopy shows little difference at these different flow rates. (e) Smoother channel walls result in similar features in the gel deposit, regardless of the micron scale roughness.

5.1 Additional notes on included video

There is a slight time delay between the moment when the ablated alginate gel leaves the field of view and the pressure drops. There are at least two reasons for this. The view in the video represents only the first tenth of the channel: at least 0.5s is needed for flow to reach the end of the channel and the piece of gelled alginate to completely exit the device. Secondly, the response time of the control system of the pump is $\sim$2s: whenever an ablation event causes an increase in flow rate above the fixed set point, the pump then counteracts this by lowering the driving pressure. This response takes $\sim$2s.

A partial ablation event is seen at 0:22-0:23. A portion of deposited gel, downstream of the main deposit, breaks off of the channel wall and is eluted from the device. As a result, the driving pressure plateaus for $\sim$1s ($\sim$5s in real time). Then, the gel deposit continues to grow and obstruct the channel, requiring higher driving pressures. A similar partial ablation event is seen at the end of the video (0:57).

To provide a comparison of the time scales involved in the flow, we note that there is a wave of growing gel that moves perpendicular to the flow direction. This occurs within the first 5s of the video, at a location approximately 100 μm downstream of the junction. This wave moves ~ 10 μm in the transverse direction over ~ 10s. This motion is much slower than the linear velocity of the fluid flowing past at 20 mm/s.

6 Confocal z-stack microscopy

To help visualize the location of the alginate gel deposit in the z-direction, clay is suspended in the alginate solution in a flow test where $C_{Alg} = 0.1$ mg/mL, $C_{Ca^{2+}} = 100$ mM and $Q_T = 2.4 \mu$L/min. Because the linear velocity through the device is so fast (40mm/s), only stationary clay pieces can be imaged clearly. Confocal z-stack microscopy reveals pieces of clay which are in-focus at different heights within the channel. SI Fig. 8 shows two images of deposited gel in a channel at different heights within the device, each 5μm away from glass slide 'floor' and the PDMS 'ceiling', respectively. The images show that clay pieces are caught in alginate gel throughout the channel volume, from top to bottom in the z-direction; alginate deposition is not limited to the bottom wall of the channel only.
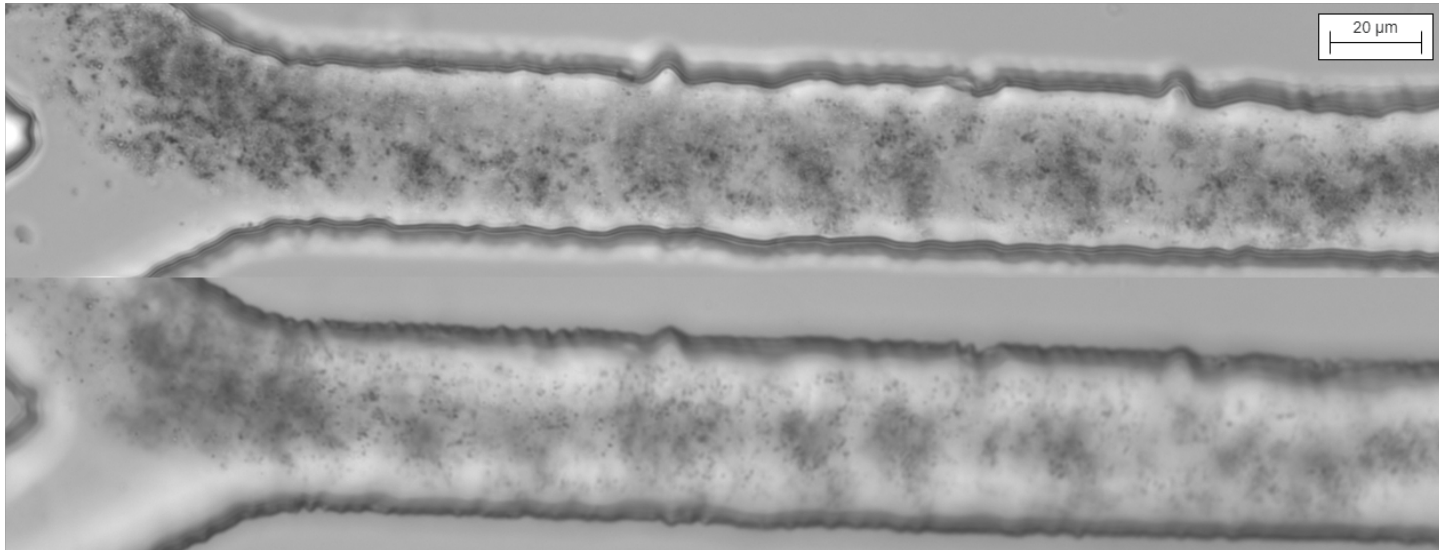

Figure 8: Confocal z-Stack microscopy shows that clay pieces are caught in the gel both near the top and bottom walls of the channel. In the top image, the plane of focus is 5μm above the channel 'floor', while in the bottom image, the plane of focus is 5μm below the channel 'ceiling.' Clay pieces embedded in the gel deposit can be seen in focus in both images, demonstrating that alginate gel deposits throughout the device.

7 Effect of gravity

While the results seen in SI Fig. 8 suggest that gravity does not play an important role in the alginate deposition, we confirm this by standing a device upright in the z-direction, with flow driven either with or against the force of gravity. A device is fixed in different orientations with respect to gravity while flowing alginate and calcium at $C_{Alg} = 0.1$ mg/mL, $C_{Ca^{2+}} = 100$ mM and $Q_T = 1.2 \mu$L/min. SI Fig. 9 shows two traces of $\Delta P(t)$ obtained at the two different orientations of the device. In the trace labeled 'Outlet Up,' the pump drives flow against gravity, while in the trace labeled 'Outlet Down,' the pump drives flow with gravity. If gravity were a significant force, we would expect the intermittent flow behavior to vary based on whether the outlet is above or below the rest of the device. We see no difference between the behavior of $\Delta P(t)$ obtained from the two different device orientations, revealing that gravity is not a significant cause of gel deposition and clog formation.
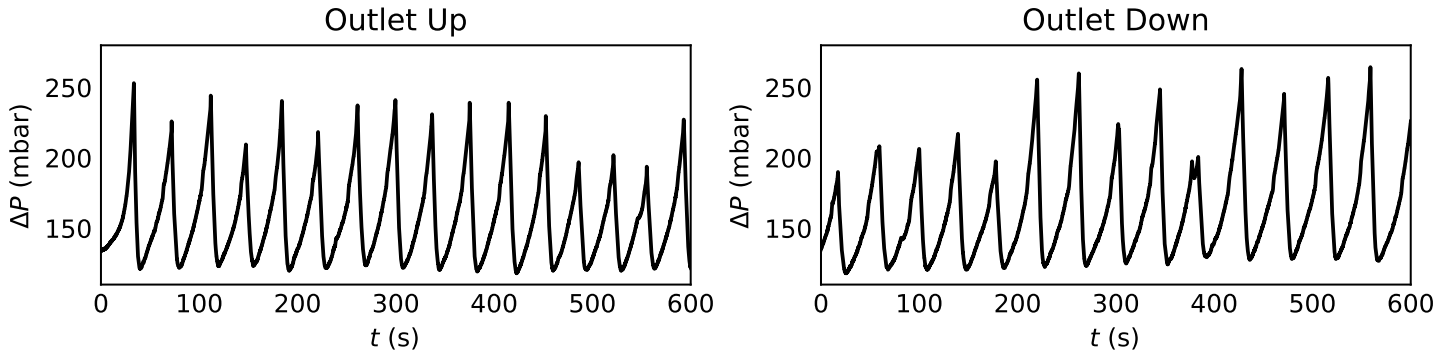
Figure 9: The plots show the behavior of intermittent flow when a device is oriented in the upright direction, with flow driven either against ('Outlet Up') or with ('Outlet Down') gravity. The flow behavior is the same in both cases, demonstrating that gravity is not a significant force for gel deposition. Data is taken at $C_{Alg} = 0.1$ mg/mL, $C_{Ca^{2+}} = 100$ mM and $Q_T = 1.2\mu$L/min.

8 Microrod production and intermittent behavior occurs at different flow rate ratios

We find that the production of rods does not depend strong on the flow rate ratio between alginate and calcium. Rods produced at a flow rate ratio of 4:1 alginate:calcium (as seen in sI Fig. 10) do not differ greatly in appearance with those produced at a 1:1 flow rate ratio (as shown in Figure 2 of the main manuscript). At both conditions, rods form that are 30μm wide and several hundred micron in length.

Also present in the effluent are pieces of alginate gel with no discernible shape, as seen in the background of image (b). Notably, these pieces do not visibly leave the device, but develop over time in the eluted solution. We suspect therefore that these pieces represent alginate which did not react within the device but only after elution.
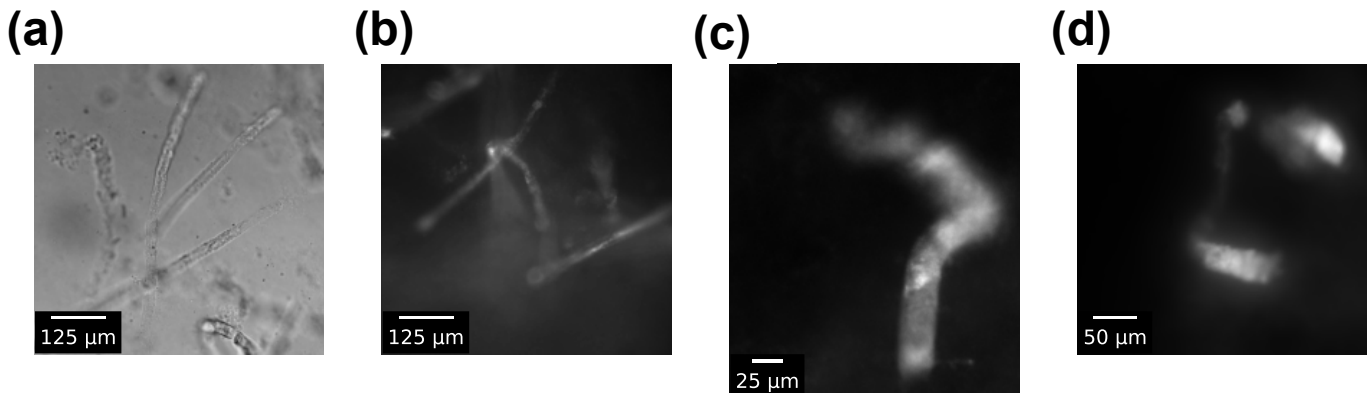

Figure 10: Additional microscopic images of eluted rods. Image (a) was taken using phase contrast microscopy, while images (b-c) use fluorescent microscopy to image embedded fluorescent particles. Images (a) and (b) were taken at 5x magnification and each show several rods that have not been separated from the eluted solution. Images (c) and (d) each show a single rod taken at 20x magnifaction.
Rods were produced at $C_{Alg} = 0.1$ mg/mL, $C_{Ca^{2+}} = 100$ mM and $Q_T = 1.2\mu$L/min at a 4:1 Alginate:Calcium flow rate ratio.

9 Clogging at high alginate concentration can be overcome by flowrate

Conditions $C_{Alg} = 10$ mg/mL and $Q_T = 1.2\mu$L/min result in complete clogging at high concentrations of calcium, conditions which fall within the red shaded region of Fig. 4 in the manuscript. For instance, SI Fig. 11 shows $\Delta P(t)$ when $C_{Ca^{2+}} = 1000$ mM, in blue. As a comparison, $\Delta P(t)$ is also plotted for a low calcium concentration, $C_{Ca^{2+}} = 0.5$ mM, in orange. The difference between the two traces is clear: low calcium results in pure, undisturbed flow, while a great excess of calcium

causes the pump to reach the maximum value of $\Delta P = 2000$ mbar and the flow test to fail. In this case, no fluid passes through the device despite the pump reaching the maximum driving pressure.

We observe that intermittent behavior reappears upon increasing the flow rate. SI Fig. 12 shows $\Delta P(t)$ obtained at $C_{Alg} = 10$ mg/mL and $C_{Ca^{2+}} = 20$mM. In Fig. 4 in the manuscript, this composition falls well within the red shaded region obtained when $Q_T = 1.2\mu$L/min. However, at a higher flow rate $Q_T = 6.0\mu$L/min, as in SI Fig. 12, a permanent clog does not form and instead the condition exhibits the intermittent deposition/ablation pattern.
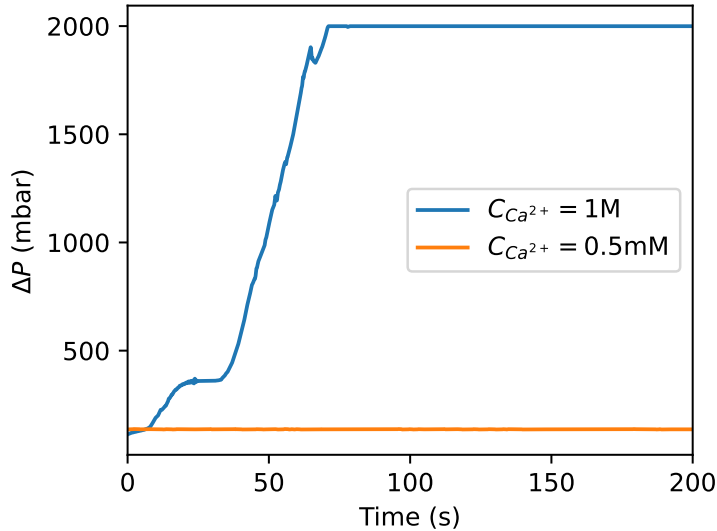

Figure 11: At high concentrations of calcium, complete clogging of the channel occurs at $Q_T = 1.2\mu$L/min and $C_{Alg} = 1$ mg/mL, as shown in blue, when $C_{Ca^{2+}} = 1000$ mM. No deposition is seen, however, when the calcium concentration is low, $C_{Ca^{2+}} = 0.5$ mM, as seen in orange.
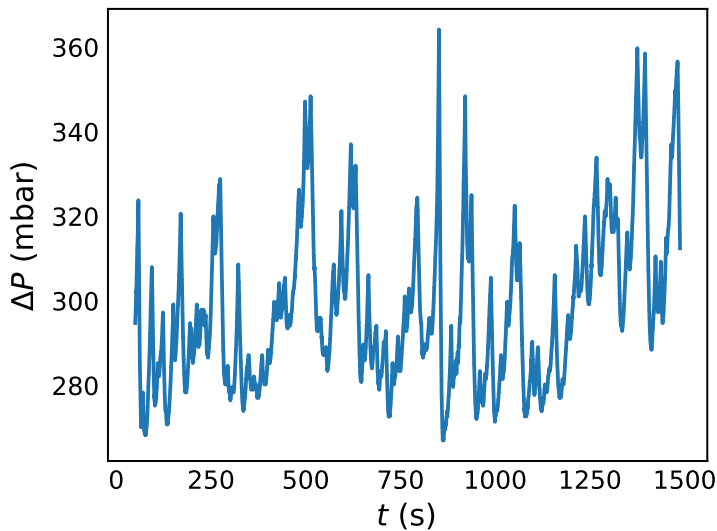

Figure 12: Intermittent deposition behavior is seen in alginate flows crosslinked by high concentrations of calcium, provided the flow rate is sufficiently high. The plot of $\Delta P(t)$ represents data taken at $C_{Alg} = 10$ mg/mL, $C_{Ca^{2+}} = 20$ mM and $Q_T = 6.0\mu$L/min.

References

(1) Dodero, A.; Vicini, S.; Alloisio, M.; Castellano, M. *Rheologica Acta* **2020**, *59*, 365–374.

(2) Larsen, B. E.; Bjørnstad, J.; Pettersen, E. O.; Tønnesen, H. H.; Melvik, J. E. *BMC biotechnology* **2015**, *15*, 1–12.

(3) LeRoux, M. A.; Guilak, F.; Setton, L. A. *Journal of Biomedical Materials Research: An Official Journal of The Society for Biomaterials, The Japanese Society for Biomaterials, and The Australian Society for Biomaterials and the Korean Society for Biomaterials* **1999**, *47*, 46–53.

(4)   Trantidou, T.; Elani, Y.; Parsons, E.; Ces, O. *Microsystems & nanoengineering* **2017**, *3*, 1–9.

(5)   Abate, A. R.; Lee, D.; Do, T.; Holtze, C.; Weitz, D. A. *Lab on a Chip* **2008**, *8*, 516–518.